Majalah Obat Tradisional (Trad. Med. J.), September-December 2024
Vol. 29(3), p 276-285
ISSN-p : 1410-5918 ISSN-e : 2406-9086

Submitted : 09-11-2023
Revised : 01-06-2024
Accepted : 03-12-2024

Mauli Banana Stem Gel: A Potential Material for Dentin Remineralization Analyzed Using Fourier Transform Infrared Spectroscopy

Amy Nindia Carabelly[1]*, Yajma Kamiila Rahman[2], Dewi Puspitasari[3], Isyana Erlita[4], Erida Wydiamala[5]

[1] Department of Oral Pathology and Maxillofacial, Faculty of Dentistry, Lambung Mangkurat University, Banjarmasin, South Kalimantan, Indonesia
[2] Dental Faculty Student, Lambung Mangkurat University, Banjarmasin, South Kalimantan, Indonesia
[3] Department of Dental Material, Faculty of Dentistry, Lambung Mangkurat University, South Kalimantan, Banjarmasin, Indonesia
[4] Department of Conservative Dentistry, Faculty of Dentistry, Lambung Mangkurat University, Banjarmasin, South Kalimantan, Indonesia
[5] Department of Parasitology, Faculty of Medical, Lambung Mangkurat University, Banjarmasin, South Kalimantan, Indonesia

ABSTRACT

Dental caries requires remineralizing agents to restore the dentin. Mauli banana stem gel is predicted to be an alternative material for mineral deposition during the remineralization process. Fourier transform infrared spectroscopy (FTIR) can analyze substances that indicate dentin remineralization. This study aimed to conduct an FTIR analysis of Mauli banana stem gel as a potential substitute material for dentin remineralization. The study utilized dentin slices obtained from the first premolars of the maxilla, which were demineralized using EDTA. Subsequently, the dentin slices were treated with CPP-ACP, 50% MBSG, 62,5% MBSG, and artificial saliva. A test tube containing 15 ml of artificial saliva was placed inside the smeared material, which was applied twice a day. It was left for three minutes and then rinsed with deionized water before being incubated at 37 °C. Basting was carried out for 21 days, and FTIR observations were performed. The major absorbance peaks detected were O-H and N-H stretch; C-H stretch; SCN stretch; Amide I; CO32-(v3) and collagen; Amide II; CH2 scissoring; C-H deformation; C-H stretching; Amide III; and PO43-(V3). MBSG demonstrated superior retention of dentin collagen compared to the control group, but it could not maintain the mineral content level on day 21. MBSG demonstrated a decrease in crystallinity due to a rise in carbonate content in the hydroxyapatite lattice. The study's findings indicate that MBSG remains unsuitable for dentin remineralization. Additional additives are necessary to enhance the levels of collagen and minerals in remineralized dentin.

Keywords: Caries; FTIR; Mauli banana stem gel; Remineralization

INTRODUCTION

Cavities are a symptom of dental caries, an infectious condition that affects the hard tissues of the teeth (Sari et al., 2017; Sumual et al., 2016). According to the Global Burden of Disease (GBD), two billion people worldwide suffer from dental caries in their permanent teeth (Agung & Palgunadi, 2022). Health Research reports that the prevalence rate of dental caries in South Kalimantan is 46.9%, somewhat higher than Indonesia's figure of 45.3% (Kemenkes RI, 2018). Untreated dental caries will cause dentin demineralization, which will worsen over time (Al-Falah et al., 2022).

Remineralization is necessary to repair demineralized dentin. Casein phosphopeptide-amorphous calcium phosphate (CPP-ACP) is a widely used remineralizing agent (Zhou et al., 2020). CPP-ACP functions by transporting calcium and phosphate ions to the area of tooth demineralization (Dwiandhono et al., 2019; Zhou et al., 2020). Discovering natural components as a substitute for CPP-ACP is crucial due to its limitations for individuals with lactose intolerance. The Mauli banana plant is one of many easily accessible herbal compounds with few adverse effects (Amin et al., 2022; Cardoso et al., 2020).

The Mauli banana plant (Musa acuminata) naturally thrives in South Kalimantan. Mauli banana stem gel has the highest content of tannins, up to 67.59% (Apriasari et al., 2020). Proanthocyanidin (PA) is a type of tannin that acts as a collagen cross-linker. It enhances the dentin matrix's stability by protecting the collagen fibrils from degradation and preventing mineral dissolution (Epasinghe et al., 2016). Ensuring the

***Corresponding author : Amy Nindia Carabelly**
Email : amy.carabelly@ulm.ac.id

DOI: 10.22146/mot.90537| *Majalah Obat Tradisional, 29(3), 2024*

stability of the demineralized dentin matrix is crucial for preventing mineral loss and facilitating mineral deposition throughout the remineralization process (Epasinghe et al., 2016). Researchers hypothesized that Mauli banana stem gel may serve as a substitute material for remineralizing dentin. Fourier transform infrared (FTIR) spectroscopy can be utilized to analyze the chemical composition indicating dentin remineralization (Zhou et al., 2020). This study aimed to conduct an FTIR analysis of Mauli banana stem gel as a potential substitute material for dentin remineralization.

MATERIALS AND METHODS

Materials

The materials used in this study included Ethylenediaminetetraacetic acid (EDTA) (PREVEST DenPro®), 70% Ethanol (Veeklin), Potassium dichromate compound ($K_2Cr_2O_7$) (Merck), Propylene glycol (Merck), Glycerin (Merck), Na-CMC (HIMEDIA®), Nipagin (Golden Era), Aquades (Smart Lab), $CaCl_2$ (Merck), KH_2PO_4 (Merck), Hepes (HIMEDIA®), NaCl (Merck), Deionized water (OneMed), and CPP-ACP (GC Tooth Mousse™).

The instrument used in this research included Ultrasonic cleaner (Vortex Mixer VM-300, Gemmy), Low-speed diamond saw (IsoMet Lowspeed Diamond Saw, Buehler), Carbide polishing paper (FORCIPOL 202, Metkon), Oven (Climate Standards Enviromental Oven, LIB™), and Rotary vacuum evaporator (Vacum rotary Evaporator N-1110S, EYELA®).

Methods

This study was granted research ethics permission from the Faculty of Dentistry at Lambung Mangkurat University in Banjarmasin, Indonesia, with No.083/KEPKG-FKGULM/EC/VII/2022. It employed a true-experimental, pure experimental research methodology.

Preparation of dental samples

The sample for this study consisted of human maxillary first premolars that met specific requirements, including being caries-free, having no restorations, having intact crowns and roots, and having been extracted within the past three months. The exclusion criteria comprised maxillary first premolar teeth with fractured crowns and roots, and teeth that had undergone bleaching. Prior to that, teeth were rinsed in an ultrasonic cleaner with a deionized solution for five minutes. Afterward, the teeth underwent preparation using a low-speed diamond saw to 4x4x1 mm, and were polished using carbide polishing paper with grits of 180, 400, 800, 1200, 1500, and 2000 (Zhou et al., 2020). The dentin slices were rinsed in an ultrasonic cleaner with a deionized solution for five minutes to remove the smear layer. After that, the dentin slices were demineralized by immersing them in an Ethylenediaminetetraacetic acid (EDTA) solution containing 17% EDTA for 72 hours (Srisomboon et al., 2021).

Preparation of Mauli banana stem extract gel

Mauli banana plants used in this study have been subjected to variety determination at the FMIPA Banjarbaru Laboratory in South Kalimantan, Indonesia. The Mauli banana stems were 15 to 21 weeks old, the plant had undergone flowering, the fruit appeared fully developed, and the stalk had fallen. The extracted Mauli banana stem portion was located 10 cm from the root weevil (Suwanto. et al., 2017; Wahyudi et al., 2022). Mauli banana stems were sliced and then dried in an oven at 40–60 °C for three days. Mauli banana stems were macerated in a 70% ethanol solution for three days until the ethanol solution surpassed the sample surface. A daily screening was conducted (Wahyudi et al., 2022). Dried Mauli banana stems were mashed using a blender to obtain simplisia powder, which will then be extracted. The extraction process was carried out using the maceration method. Mauli banana stems simplisia powder was immersed in a 70% ethanol solution maintained at 1 cm above the sample surface. The mixture was agitated and filtered daily for three days. A rotary vacuum evaporator was employed to generate a viscous extract at temperatures lower than 40–50 °C (Wahyudi et al., 2022). The concentration of ethanol in the Mauli extract was determined using the potassium dichromate compound ($K_2Cr_2O_7$) (Ananda et al., 2018). Free extracts will not undergo discoloration when given reagents (Ananda et al., 2018). The Mauli banana extract gel (MBSG) was made by mixing Mauli banana stem extract, propylene glycol, glycerin, Na-CMC, nipagin, and aquades until 50% and 62.5% concentrations were achieved (Wahyudi et al., 2022). The artificial saliva was prepared by combining 1.5 mmol/L $CaCl_2$, 0.9 mmol/L KH_2PO_4, 20 mmol/L Hepes, and 150 mmol/L NaCl (Zhou et al., 2020).

Dentin Treatment

The demineralized dentin slices were then given four different treatments. The first treatment group (control group) was dentin slices rinsed using deionized water and inserted into a test tube containing 15 mL of artificial saliva incubated at

37°C. The artificial saliva was replaced every 24 hours for 21 days. On the 21st day, dentin slices were washed with deionized water using an ultrasonic cleaner for two minutes (Zhou et al., 2020). The dentin slices in the second treatment group (CPP-ACP group) were subjected to CPP-ACP application. The third treatment group (MBSG1 group) was dentin slices applied to 50% Mauli banana stem gel, and the fourth treatment group (MBSG2 group) was dentin slices applied to 62.5% Mauli banana stem gel. CPP-ACP and MBSG smearing was carried out twice a day, which was allowed to stand for three minutes, then rinsed using deionized water and transferred into a test tube containing 15 mL of artificial saliva and incubated at 37°C. Basting was carried out for 21 days. Artificial saliva was replaced with each MBSG or CPP-ACP application. On day 21, dentin slices were cleaned with deionized water using an ultrasonic cleaner for two minutes (Zhou et al., 2020).

Fourier Transform Infrared Spectroscopy (FTIR) analysis

The FTIR analysis was performed using FT-IR (Thermo Scientific Nicolet iS20, United States). The FTIR band observations were acquired using Origin software. Molecular interactions with infrared waves were observed at wavenumbers of 4000-400 cm^{-1}. The resulting data were spectra, which include absorbance and wavenumbers.

In addition, the following parameters were calculated from the area ratios: (1) Ratio of mineral to matrix (band area ratio: $PO_4^{-3}{}_{(v3)}$/Amide I; $PO_4^{-3}{}_{(v3)}$/Amide II; and $PO_4^{-3}{}_{(v3)}$/ Amide III) (Lopes et al., 2018); (2) Ratio of Amide I to Amide II (band area ratio: Amide I/Amide II)(Lopes et al., 2018); (3) Ratio of carbonate to phosphate (band area ratio: $CO_3^{2-}{}_{(V3)}$ / $PO_4^{-3}{}_{(v3)}$)(Lopes et al., 2018).

RESULTS

Table I shows the absorbance peaks detected for dentine from the control group, CPP-ACP group, MBSG1 group, and MBSG2 group. Absorbance bands at 3200-3400 cm^{-1} represent O-H and N-H stretch. Absorbance bands at 2850-3000 cm^{-1} represent the C-H stretch. Absorbance bands at 2175–2140 cm^{-1} represent SCN stretch. Absorbance bands at 1600–1700 cm^{-1} represent Amide I. Absorbance bands at 1410–1640 cm^{-1} represent $CO_3^{2-}{}_{(V3)}$ overlapped with collagen. Absorbance bands at of 1525-1554 cm^{-1} represent Amide II. Absorbance bands at 1450 cm^{-1} represent CH_2 scissoring. Absorbance bands at 1420-1380 cm^{-1} represent C-H deformation. Absorbance bands at 1337 cm^{-1} represent C-H stretching. Absorbance bands at of 1286-1216 cm^{-1} represent Amide III. Absorbance bands at 1000-1100 cm^{-1} represent $PO4^{3-}{}_{(V3)}$.

Figure 1 shows typical absorbance peaks at 3200-3400 cm^{-1} represent hydroxyl and amine groups (O-H and N-H stretch) (a)**;** absorbance peaks at 2850-3000 cm^{-1} represent C-H stretch (b); and absorbance peaks at 2175-2140 cm^{-1} represent C-H stretch (c)**.** The absorbance peaks of O-H and N-H stretch (a) in MBSG1 and MBSG2 were higher than the control and CPP-ACP groups. The absorbance peak width of C-H stretch (b) in MBSG1 and MBSG2 was higher than the control and CPP-ACP groups, while the control and CPP-ACP groups had nearly the same peak. The absorbance peak of SCN stretch (c) in MBSG1 and MBSG2 was higher than control and CPP-ACP groups, though the MBSG 1 and MBSG 2 had nearly the same peak.

Figure 2 shows the absorbance peaks for the dentine proteins, which are represented by Amide I (1600-1700 cm^{-1}) and $CO_3^{2-}{}_{(V3)}$ overlapped with collagen (1410-1640 cm^{-1}) (d) (Lopes et al., 2018), Amide II (1525-1554 cm^{-1}) (e) (Karteva & Manchorova, 2019), Amide III (1286-1216 cm^{-1}) (i) (Lopes et al., 2018), and -CH_2-scissoring (1450 cm^{-1}) (f) (Lopes et al., 2018). The absorbance peaks for the mineral, which is represented by phosphate at 1000-1100 cm^{-1} ($PO_4^{3-}{}_{(V3)}$) (j) (Lopes et al., 2018). Other absorbancies were found at 1410-1640 cm^{-1} ($CO_3^{2-}{}_{(v3)}$ overlapped with collagen) (d) (Lopes et al., 2018), 1420-1380 cm^{-1} (C-H deformation) (g) (Martínez-Castaño et al., 2020), 1337 cm^{-1} (C-H stretching) (h) (Tang et al., 2023). Figure 2 shows that the absorbance peaks of amide I (d), amide II (e), -CH2-bending vibrations (f), C-H deformation (g), C-H stretching (h), and amide III (i) were higher in the MBSG group than in the control and CPP-ACP groups. However, the absorbance peaks of phosphate in MBSG1 and MBSG2 were higher than in the CPP-ACP and control groups.

The mineral-to-matrix ratio was determined by calculating the ratios of phosphate to amide I, phosphate to amide II, and phosphate to amide III in all treatments (Figure 3). This ratio was utilized to analyze the distribution of mineral concentration in the dentin sample. The CPP-ACP group exhibited the highest mineral concentration, with the control groups, MBSG1, and MBSG2 following in descending order.

Figure 4 displays the ratio between amide I to amide II for all treatments. The ratio of amide I to amide II determines the orientation of the collagen fibers. Based on the findings, the CPP-ACP group exhibited the highest number of collagen fibers, followed by the MBSG2, MBSG1, and control groups. This indicates that the CPP-ACP group has the highest collagen levels. Compared to the CPP-

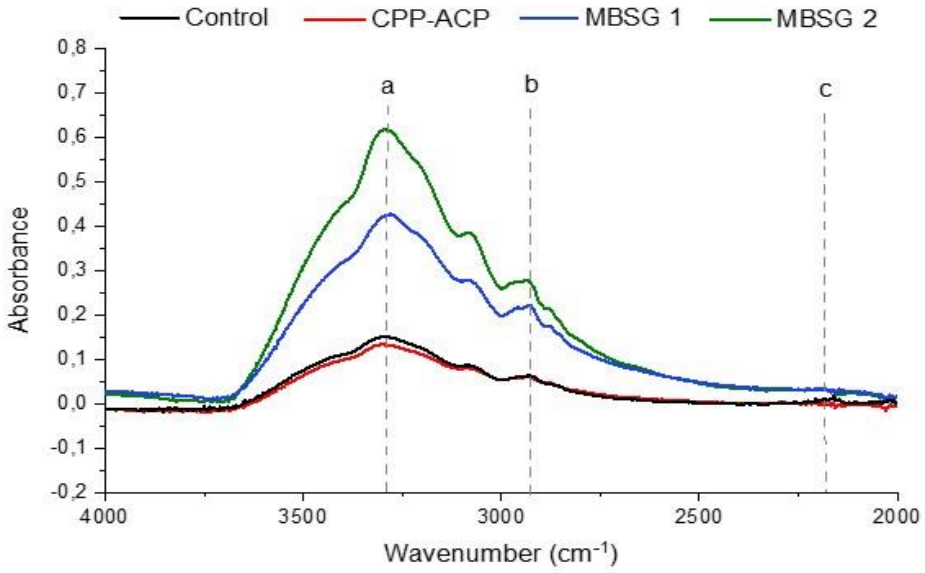

(a = O-H stretch, N-H stretch; b= C-H stretch; c= SCN stretch)

Fig 1. FTIR spectra at 4000-2000 cm^{-1} of control groups, CPP-ACP groups, Mauli Banana Stem Gel 50% (MBSG 1), and Mauli Banana Stem Gel 62,5% (MBSG 2).

Table I. The mayor FTIR peaks detected for control groups, CPP-ACP groups, Mauli Banana Stem Gel 50% (MBSG 1), and Mauli Banana Stem Gel 62,5% (MBSG 2)

Sample	O-H and N-H	C-H	SCN	AMIDE 1	CO_3^{2-} (V3) overlapped with colagen	AMIDE II	CH_2 scissoring	C-H deformation	C-H stretching	AMIDE III	PO_4^{-3} (V3)
Control	3296	2928	2161	1629	1620	1541	1451	-	1336	1237	1031
CPP-ACP	3296	2940	-	1634	1634	1539	1454	-	1337	1234	1029
MBSG 1	3281	2929	-	1651, 1633	1651, 1633	1538	1454	1393	1337	1235	1079
MBSG2	3295	-	-	1633	1633	1539	1454	1397	1337	1236	1080
Reference	3200-3400 (Pavia et al., 2014)	2850-3000 (Pavia et al., 2014)	2175-2140 (Nandiyanto et al., 2019)	1600-1700 (Lopes et al., 2018)	1410-1640 (Lopes et al., 2018)	1525-1554 (Karteva & Manchorova, 2019)	1450 (Lopes et al., 2018)	1420-1380 (Martínez-Castaño et al., 2020)	1337 (Tang et al., 2023)	1286-1216 (Lopes et al., 2018)	1000-1100 (Lopes et al., 2018)

ACP group, the MBSG group could not match the amount of collagen in the dentin.

Figure 5 shows the ratio between carbonate to phosphate for all treatment groups. The carbonate-to-phosphate ratio indicates the degree of carbonate incorporation into the hydroxyapatite lattice. The MBSG2 group exhibited the highest value, followed by the MBSG1, control, and CPP-ACP groups. This suggests that the MBSG group contains a higher concentration of carbonate ions within the hydroxyapatite lattice compared to the control and CPP-ACP groups.

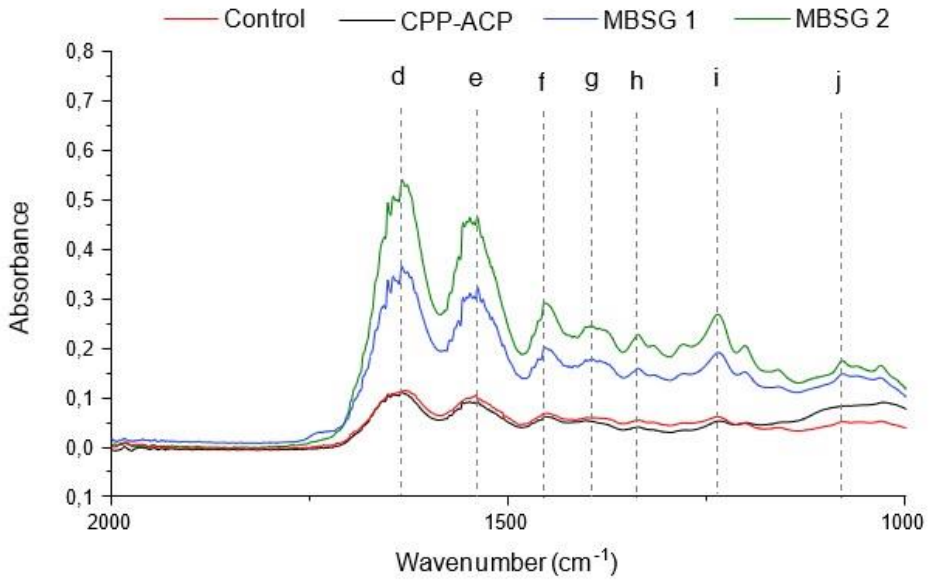

(d = Amide I, $CO_3^{2-}{}_{(V3)}$ overlapped with colagen; e = Amide II; f = -CH_2-bending vibrations; g = C-H deformation; h = C-H streching; i = Amide III; j = $PO_4^{3-}{}_{(V3)}$)

Figure 2. FTIR spectra at 2000-1000 cm^{-1} of control groups, CPP-ACP groups, Mauli Banana Stem Gel 50% (MBSG 1), and Mauli Banana Stem Gel 62,5% (MBSG 2).

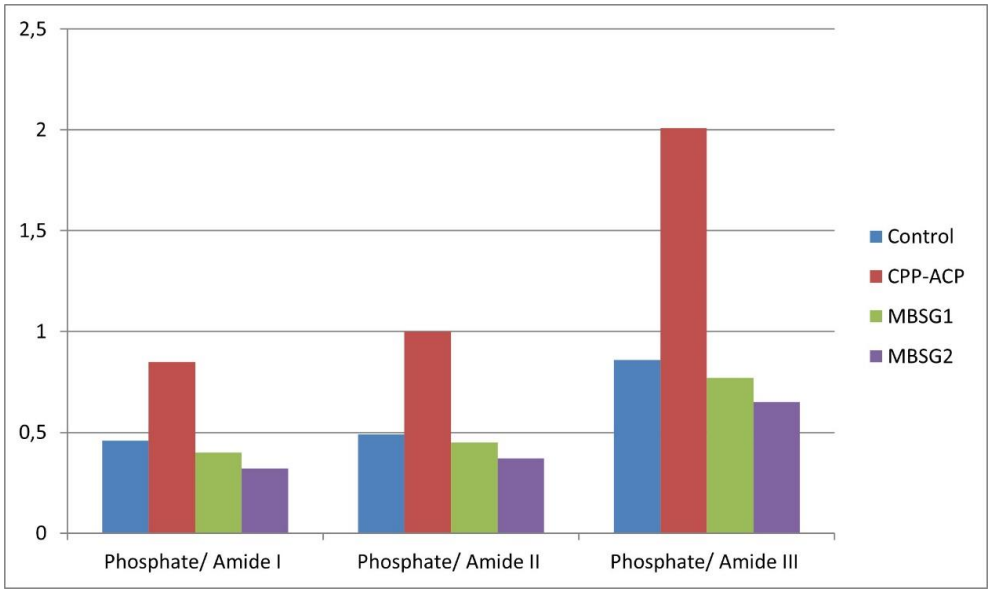

Figure 3. Ratio of mineral to matrix in all treatment groups

DISCUSSIONS

Dentin comprises 70% minerals, 20% organic matter, and 10% water (Lopes et al., 2018). Calcium and phosphate are the most abundant minerals in dentin, while type 1 collagen is the most abundant organic matter (Lopes et al., 2018). Mineral deposition into and between collagen fibrils forms a hard, tough, and resistant matrix. Dentin caries leads to the demineralization of mineral content and collagen degradation (Lopes et al., 2018). MBSG is a potential material for remineralizing dentin that can be studied using FTIR analysis. The composition and number of chemical compounds required for a material to reach its potential can be determined using FTIR, one of the X-ray diffraction techniques (Karteva & Manchorova, 2019).

This study's findings showed an absorbance peak at 1000-1100 cm^{-1}, which was identified as a $PO_4^{3-}{}_{(V3)}$ or phosphate (Lopes et al., 2018).

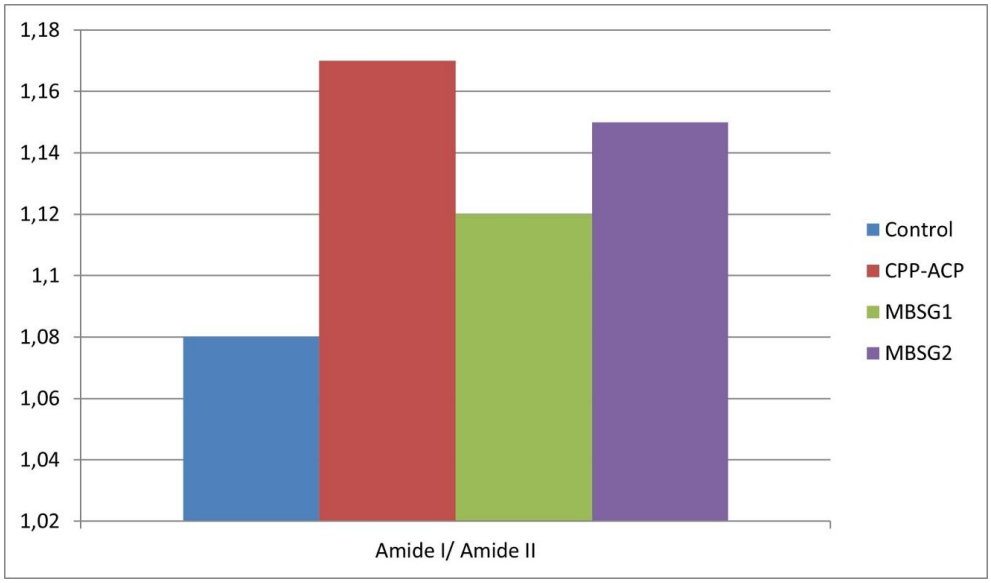

Figure 4. Ratio of amide I to amide II in all treatment groups

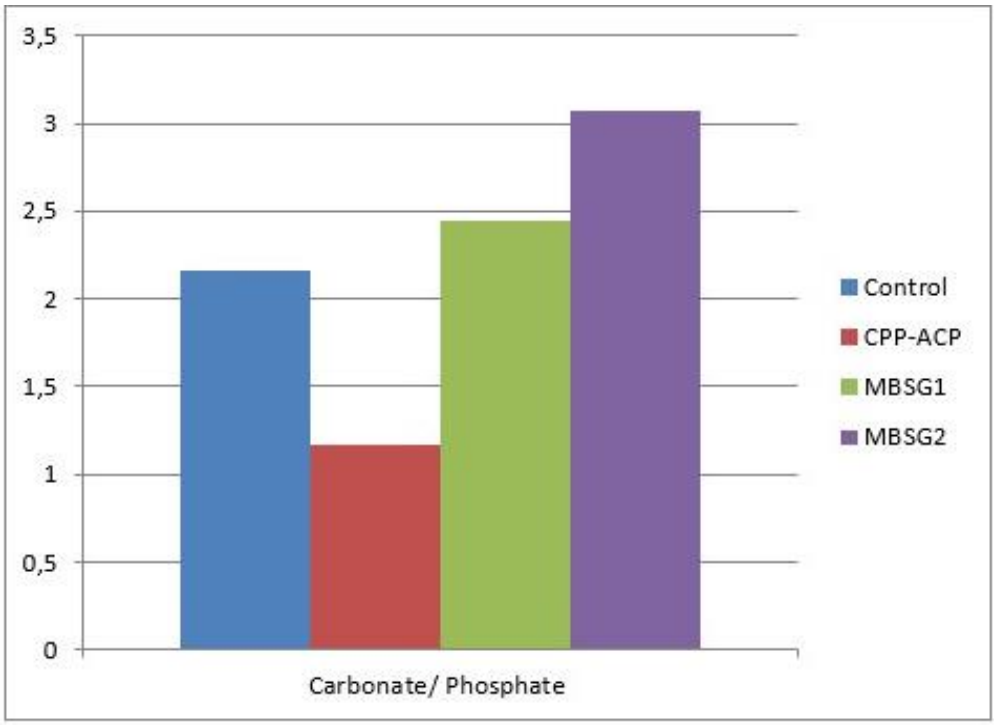

Figure 5. Ratio of carbonate to phosphate in all treatment groups

Phosphate contributes to forming a strong dentin mineral skeleton, which impacts dentin's mechanical characteristics and strength. When dentin is demineralized, the phosphate in the dentin matrix is released. The phosphate can be released due to bacterial acids or other demineralization processes (Rodrigues et al., 2018). In this study, the absorbance peak of phosphate in MBSG1 and MBSG2 was higher than in the CPP-ACP and control (Figure 2).

Type I collagen is the most abundant organic component in dentin (90%) (Lopes et al., 2018). Collagen is responsible for the fibrillar matrix's mechanical properties, including tensile strength and viscoelasticity (Lopes et al., 2018). Type I collagen is presented in FTIR as amide I (1600-1700 cm^{-1}), amide II (1525-1554 cm^{-1}), and amide III (1286-1216 cm^{-1}) (Karteva & Manchorova, 2019; Lopes et al., 2018). Amide I involves C=O bonds; amide II involves N-H and C-N bonds in

peptide bonds; and amide III involves C-N and C-C bonds (Lopes et al., 2018). The results of this study showed that there was amide I, II, and III in all treatment groups despite dentin demineralization (Table I). This aligns with Siyuan's research, which states that collagen represented by amides I and II remains intact even after demineralization (Pang et al., 2021). The MBSG2 group exhibited the highest absorbance peaks for amide I, II, and III, followed by the MBSG1, control, and CPP-ACP groups (Figure 2).

Collagen is represented by amide (NHCO-), C-N, C-H, C-C, and N-H bonds (Lopes et al., 2018). In this study, the C-H group was found at 2850-3000 cm^{-1} (Almhöjd et al., 2014). The MBSG 1 and MBSG 2 groups had a higher absorbance peak than the CPP-ACP and control groups (Figure 1). The functional groups N-H and O-H were also found at 3200-3400 cm^{-1} (Almhöjd et al., 2014). O-H and N-H groups can interact with collagen and other organic components through hydrogen bonding. This interaction plays a role in maintaining the structural stability of dentin (Kim et al., 2016).

In addition to collagen, dentin contains lipids and non-collagen matrix proteins as organic components. These components can be identified in the FTIR spectrum by the presence of functional groups that exhibit CH_2 scissoring (Almhöjd et al., 2014). The results findings indicated CH_2 scissoring was present in all groups. The CH_2 scissoring is a distinctive feature of the chemical bond between carbon and hydrogen in the hydrocarbon chain of the lipid. The visibility of lipids, including fats and phospholipids, in the dentin matrix is enhanced when the mineral components are removed, as indicated by the presence of the tops of the group. Goldberg states that dentin lipids can bind to minerals through lipo-or-phospho-protein bonds, forming complexes that contribute to dentin's mineralization properties and strength (Goldberg, 2021). CH_2 scissoring absorbance peaks were higher in the MBSG group compared to the control and CPP-ACP groups.

This study's findings also showed that an absorbance peak at 2175-2140 cm^{-1} represents SCN (Figure 1), an absorbance peak at 1420-1380 cm^{-1} represents C-H deformation, and an absorbance peak at 1337 cm^{-1} represents C-H stretching (Figure 2) (Martínez-Castaño et al., 2020; Nandiyanto et al., 2019). The SCN is thiocyanate, a fluid found in dentinal tubes and an indicator of pathological processes in caries (Seredin et al., 2019). In this study, thiocyanates were only found in the control group. The C-H deformation was only found in the MBSG group, while the C-H stretching was found in all treatment groups.

The phosphate and amide I ratios are used to analyze mineral content distribution (Figure 3) (Liu et al., 2014). The findings of this study indicated that the group treated with CPP-ACP exhibited the largest number of organic matrices, whereas the control group, MBSG1 and MBSG2, followed in descending order. CPP-ACP is a complex derived from milk protein that can precipitate dentin minerals such as calcium, phosphate, and fluoride (Guanipa Ortiz et al., 2019). CPP-ACP can dissociate into calcium and phosphate, which bind to the tooth surface and provide a large reservoir of calcium and phosphate. This helps to maintain a high concentration of dental minerals, keeping them in a supersaturation condition (Guanipa Ortiz et al., 2019).

Mauli banana stem gel contains ascorbic acid, β-carotene, lycopene, saponins, alkaloids, flavonoids, and tannins (Apriasari et al., 2020). The largest content of MBSG is tannins, and one type of tannin is Proantocyanidine (PA) (Boteon et al., 2017). The phenolic hydroxyl group of PA can form hydrogen bonds with the carbonyl or hydroxyl group of collagen and improve the mechanical properties of collagen fibrils (Epasinghe et al., 2016; Paik et al., 2022). The stable collagen matrix acts as a mechanical barrier, which prevents acid entry and the further loss of calcium and phosphate ions from carious lesions (Epasinghe et al., 2016). However, Epasinghe's research states that there is no evidence that PA can depose the mineral dentin, although PA can inhibit demineralization and promote remineralization (Epasinghe et al., 2016).

The ratio of amide I to amide II can be used to determine collagen fibers' orientation, as depicted in Figure 4 (Karteva & Manchorova, 2019). Figure 4 shows that the CPP-ACP group had the highest collagen fibers, followed by the MBSG2, MBSG1, and control groups. CPP-ACP is known to provide a large reservoir of calcium and phosphate. Metastable calcium phosphate solutions are proposed as another method that can improve the stability and durability of the dentin collagen matrix (Guanipa Ortiz et al., 2019; Paik et al., 2022). Although the CPP-ACP group is in a better position, the findings of this study indicate that MBSG is more effective than the control group in preserving collagen in demineralized dentin. The MMP enzyme can facilitate the degradation of dentin collagen in the demineralization process. Antioxidants can hinder MMP activity, which aids in stabilizing natural collagen (Abedi et al., 2023). Prior research has demonstrated that MBSG

functions as an antioxidant by binding its bioactive compounds with ferrous iron, hydrogen peroxide, and hydroxyl (Apriasari et al., 2020). Tannin, the constituent of MBSG, exhibits a strong attraction to type I collagen (Apriasari et al., 2020; Polassi et al., 2021). Tannins are believed to form complexes with collagen, resulting in alterations in type 1 collagen's triple helix structure. This enhances collagen's structural, thermal, and enzymatic stability (Polassi et al., 2021). Tannins are believed to inhibit proteases, exhibit an affinity to dentin collagen, serve as catalysts for collagen cross-linking, and prevent dentin matrix degradation (Polassi et al., 2021). Flavonoids are also known to be natural cross-linking agents and MMP inhibitors (Paik et al., 2022).

The carbonate-to-phosphate ratio indicates the degree of carbonate incorporation into the hydroxyapatite lattice (Figure 5) (Lopes et al., 2018). Carbonate is a phosphate replacement component in hydroxyapatite crystals, resulting in changes in hydroxyapatite lattice parameters and related physical properties (Lopes et al., 2018). Crystallinity decreases when carbonate ions are introduced into the hydroxyapatite lattice. Therefore, a rise in the ratio indicates a decrease in crystallinity (Aziz et al., 2023). The MBSG2 group had the highest ratio, followed by the MBSG1, control, and CPP-ACP groups. MBSG can decrease dentin crystallinity due to the large number of carbonate ions that replace hydroxyl and phosphate ions. This results in increased dentin solubility and decreased hardness (Huang et al., 2020). Carbonate ions in the natural hydroxyapatite lattice lowers surface energy and shrink crystal size (Aziz et al., 2023). The CPP-ACP group with the lowest ratio showed the highest crystallinity. CPP-ACP acts as an extra fibrillar particle, a reservoir of calcium and phosphate ions, and hence, it is a precursor in the synthesis of hydroxyapatite (Nimbeni et al., 2023).

CONCLUSION

The results of this study showed that MBSG was able to retain dentin collagen more efficiently than the control group at day 21. However, MBSG cannot maintain the level of dentin mineral content. Instead, it decreases the crystallinity of dentin. The study findings indicated that MBSG exhibited lower levels of collagen and minerals than the CPP-ACP group and reduced dentin crystallinity. MBSG is not effective as an agent for tooth remineralization. Additional additives are required to increase collagen and minerals in remineralized dentin.

ACKNOWLEDGEMENT

This work was supported by Lambung Mangkurat University Grant (615/UN8/PG/2023).

REFERENCES

Abedi, N., Sadat Sajadi-Javan, Z., Kouhi, M., Ansari, L., Khademi, A., & Ramakrishna, S. (2023). Antioxidant Materials in Oral and Maxillofacial Tissue Regeneration: A Narrative Review of the Literature. *Antioxidants*, *12*(594), 1–33. https://doi.org/10.3390/antiox12030594

Agung, I. G. A. A., & Palgunadi, I. N. P. T. (2022). Strategy for improving the quality of School Dental Health Efforts at Tabanan Public Health Center. *Dental Journal*, *55*(4), 215–220. https://doi.org/10.20473/J.DJMKG.V55.I4.P215-220

Al-Falah, J., Prihatiningrum, B., & Nugroho, R. (2022). Perbandingan Efektivitas Enzim Bromelain dan Enzim Papain Terhadap Degradasi Jaringan Karies Dentin Sebagai Agen Chemo-Mechanical Caries Removal. *Jurnal Kedokteran Gigi Universitas Padjadjaran*, *34*(1), 58. https://doi.org/10.24198/jkg.v34i1.34457

Almhöjd, U. S., Norén, J. G., Arvidsson, A., Nilsson, Å., & Lingström, P. (2014). Analysis of carious dentine using FTIR and ToF-SIMS. *Oral Health and Dental Management*, *13*(3), 735–744.

Amin, F., Fareed, M. A., Zafar, M. S., Khurshid, Z., Palma, P. J., & Kumar, N. (2022). Degradation and Stabilization of Resin-Dentine Interfaces in Polymeric Dental Adhesives: An Updated Review. *Coatings*, *12*(8), 1–24. https://doi.org/10.3390/coatings12081094

Ananda, A., Putri, D., & Diana, S. (2018). Daya Hambat Ekstrak Ubi Bawang Dayak (Eleutherine Palmifolia (L.) Merr) Terhadap Pertumbuhan Streptococcus Mutans (Studi In Vitro Dengan Metode Difusi). *Dentin*, *2*(1), 85–90.

Apriasari, M. L., Pramitha, S. R., Puspitasari, D., & Ernawati, D. S. (2020). Anti-Inflammatory Effect of Musa acuminata Stem. *European Journal of Dentistry*, *14*(2), 294–298. https://doi.org/10.1055/s-0040-1709944

Aziz, S., Ana, I. D., Yusuf, Y., & Pranowo, H. D. (2023). Synthesis of Biocompatible Silver-Doped Carbonate Hydroxyapatite Nanoparticles Using Microwave-Assisted Precipitation and In Vitro Studies for the Prevention of Peri-

Implantitis. *J. Funct. Biomater*, *14*(385), 1–14. https://www.ncbi.nlm.nih.gov/pmc/articles/PMC10382064/

Boteon, A. P., Kato, M. T., Buzalaf, M. A. R., Prakki, A., Wang, L., Rios, D., & Honório, H. M. (2017). Effect of Proanthocyanidin-enriched extracts on the inhibition of wear and degradation of dentin demineralized organic matrix. *Archives of Oral Biology*, *84*(October 2016), 118–124. https://doi.org/10.1016/j.archoralbio.2017.09.027

Cardoso, F., Boteon, A. P., da Silva, T. A. P., Prakki, A., Wang, L., & Honório, H. M. (2020). In Situ Effect of A Proanthocyanidin Mouthrinse on Dentin Subjected to Erosion. *Journal of Applied Oral Science*, *28*, 1–7. https://doi.org/10.1590/1678-7757-2020-0051

Dwiandhono, I., Agus Imam, D. N., & Mukaromah, A. (2019). Applications of Whey Extract and Cpp-Acp in Email Surface Towards Enamel Surface Hardness After Extracoronal Bleaching. *Jurnal Kesehatan Gigi*, *6*(2), 93–98. https://doi.org/10.31983/jkg.v6i2.5481

Epasinghe, Yiu, C., & Burrow, M. F. (2016). *Effect of flavonoids on remineralization of artificial root caries*. https://doi.org/10.1111/adj.12367

Goldberg, M. (2021). *Lipids in Enamel and Dentin : Involvement in Mineralization*. 82–90.

Guanipa Ortiz, M., Alencar, C., Freitas De Paula, B., Alves, E., Nogueira Araújo, J., & Silva, C. (2019). Effect of the casein phosphopeptide-amorphous calcium phosphate fluoride (CPP-ACPF) and photobiomodulation (PBM) on dental hypersensitivity: A randomized controlled clinical trial. *PLoS ONE*, *14*(12), e0225501. https://doi.org/10.1371/journal.pone.0225501

Huang, L., Zhang, X., Shao, J., Zhou, Z., Chen, Y., & Hu, X. (2020). Nanoscale chemical and mechanical heterogeneity of human dentin characterized by AFM-IR and bimodal AFM. *Journal of Advanced Research*, *22*, 163–171. https://doi.org/10.1016/j.jare.2019.12.004

Karteva, E., & Manchorova, N. (2019). *Root Dentin Analysis from using Fourier-Transform Infrared Spectroscopy with Attenuated Total*. *8*(5), 2123–2126. https://api.semanticscholar.org/CorpusID:198943574

Kemenkes RI. (2018). Riset Kesehatan Dasar: RISKESDAS. In *Badan Penelitian dan Pengembangan Kesehatan* (p. 674).

Kim, J. H., Han, G. J., Kim, C. K., Oh, K. H., Chung, S. N., Chun, B. H., & Cho, B. H. (2016). Promotion of adhesive penetration and resin bond strength to dentin using non-thermal atmospheric pressure plasma. *European Journal of Oral Sciences*, *124*(1), 89–95. https://doi.org/10.1111/eos.12246

Liu, Y., Yao, X., Liu, Y. W., & Wang, Y. (2014). A fourier transform infrared spectroscopy analysis of carious dentin from transparent zone to normal zone. *Caries Research*, *48*(4), 320–329. https://doi.org/10.1159/000356868

Lopes, C. de C. A., Limirio, P. H. J. O., Novais, V. R., & Dechichi, P. (2018). Fourier transform infrared spectroscopy (FTIR) application chemical characterization of enamel, dentin and bone. *Applied Spectroscopy Reviews*, *53*(9), 747–769. https://doi.org/10.1080/05704928.2018.1431923

Martínez-Castaño, M., Díaz, D. P. M., Contreras-Calderón, J., & Cabrera, C. G. (2020). Physicochemical properties of bean pod (Phaseolus vulgaris) flour and its potential as a raw material for the food industry. *Revista Facultad Nacional de Agronomia Medellin*, *73*(2), 9179–9187. https://doi.org/10.15446/rfnam.v73n2.81564

Nandiyanto, A. B. D., Oktiani, R., & Ragadhita, R. (2019). How to Read and Interpret FTIR Spectroscope of Organic Material. *Indonesian Journal of Science & Technology*, *4*(1), 97–118.

Nimbeni, B., Munaga, S., Alabsi, F. S., Khurbani, Z. H., Boreak, N., & Nimbeni, S. B. (2023). Amorphous Calcium Phosphate Based Tooth Remineralization Systems in Dentistry-A Systematic Review of in-Vitro Studies. In *J Int Dent Med Res* (Vol. 16, Issue 1). http://www.jidmr.com

Paik, Y., Kim, J.-H., Yoo, K.-H., Yoon, S.-Y., & Kim, Y.-I. (2022). Dentin Biomodification with Flavonoids and Calcium Phosphate Ion Clusters to Improve Dentin Bonding Stability. *Materials*, *15*, 1494. https://doi.org/10.3390/ma15041494

Pang, S., Su, F. Y., Green, A., Salim, J., McKittrick, J., & Jasiuk, I. (2021). Comparison of different protocols for demineralization of cortical bone. *Scientific Reports*, *11*(1), 1–10.

https://doi.org/10.1038/s41598-021-86257-4

Pavia, D. L., Lampman, G. M., Kriz, G. S., & Vyvyan, J. R. (2014). Introduction to spectroscopy. In *Tetrahedron Organic Chemistry Series* (Vol. 20, Issue C). Cengage learning. https://doi.org/10.1016/S1460-1567(00)80010-0

Polassi, M., De, T., Oliveira, S., Calheiros De Carvalho, A., Soman, L., Medeiros, M., André, T., Veiga, M., Frederico De Oliveira Graeff, C., Hortencia, A., González, M., Marcucci, M. C., Dos, S., Grecco, S., & Perlatti D'alpino, P. H. (2021). Influence of Dentin Priming with Tannin-Rich Plant Extracts on the Longevity of Bonded Composite Restorations. *The Scientific World Journal*, *2021*, 1–10. https://doi.org/10.1155/2021/1614643

Rodrigues, R. B., Soares, C. J., Junior, P. C. S., Lara, V. C., Arana-Chavez, V. E., & Novais, V. R. (2018). Influence of radiotherapy on the dentin properties and bond strength. *Clinical Oral Investigations*, *22*(2), 875–883. https://doi.org/10.1007/s00784-017-2165-4

Sari, A. D., Fazrin, I., & Saputro, H. (2017). Pemberian Motivasi Orang Tua Dalam Menggosok Gigi Pada Anak Usia Prasekolah Terhadap Timbulnya Karies Gigi. *Journal Of Nursing Practice*, *1*(1), 33–39. https://doi.org/10.30994/jnp.v1i1.20

Seredin, P., Goloshchapov, D., Ippolitov, Y., & Vongsvivut, J. (2019). Spectroscopic signature of the pathological processes of carious dentine based on FTIR investigations of the oral biological fluids. *Biomedical Optics Express*, *10*(8), 4050. https://doi.org/10.1364/boe.10.004050

Srisomboon, S., Kettratad, M., Pakawanit, P., Rojviriya, C., Phantumvanit, P., & Panpisut, P. (2021). Effects of different application times of silver diamine fluoride on mineral precipitation in demineralized dentin. *Dentistry Journal*, *9*(6). https://doi.org/10.3390/dj9060070

Sumual, I. A., Pangemanan, D. H. C., & Wowor, V. N. S. (2016). Keparahan Karies Gigi yang tidak Dirawat pada Siswa SD GMIM 31 Manado Berdasarkan Indeks PUFA. *E-GIGI*, *4*(2). https://doi.org/10.35790/eg.4.2.2016.13937

Suwanto., Zahroh, R., & Fatmawati, L. (2017). Efikasi pisang (Musa paradisiaca L.) sebagai tanaman obat. In *Pokjonas Toi* (Vol. 3, pp. 79–83).

Tang, L., Zhu, L., Liu, Y., Zhang, Y., Li, B., & Wang, M. (2023). Crosslinking Improve Demineralized Dentin Performance and Synergistically Promote Biomimetic Mineralization by CaP_PILP. *ACS Omega*, *8*, 14410–14419. https://doi.org/10.1021/acsomega.2c07825

Wahyudi, M. D., Syahrina, F., Carabelly, A. N., & Puspitasari, D. (2022). Formulasi dan Uji Stabilitas Fisik Gel Ekstrak Batang Pisang Mauli (Musa acuminata). *Dentin Jurnal Kedokteran Gigi*, *4*(3), 161–165.

Zhou, Z., Ge, X., Bian, M., Xu, T., Li, N., Lu, J., & Yu, J. (2020). Remineralization of dentin slices using casein phosphopeptide-amorphous calcium phosphate combined with sodium tripolyphosphate. *BioMedical Engineering Online*, *19*(1), 1–14. https://doi.org/10.1186/s12938-020-0756-9